Air Flow Simulation Through the Stack of Onions During Storage Using Computational Fluid Dynamics

Ira Ayuningsih, An N. F. Rahmah, Devi Priyanti, Joko N. W. Karyadi, and Bayu Nugraha(✉)

Department of Agricultural and Biosystem Engineering, Universitas Gadjah Mada, Jl. Flora No. 1, Bulaksumur, Yogyakarta 55281, Indonesia
bayu.nugraha@ugm.ac.id

Abstract. The storage of 'perishable' horticultural products, such as onions (*Allium cepa* L.), must be equipped with an even air distribution. Uniform airflow in the product stack is important for quality maintenance. However, the air velocity in most of the storage space used in each part of the product stack is unknown. This study aims to measure air distribution conditions among product stacks inside the storage box. In addition, it is important to know the effect of mesh and inlet velocities on air distribution. The velocity distribution of airflow is measured by computational fluid dynamics (CFD) through the geometric approach of onions to spherical shapes. At different points inside the onion-filled storage box, the air velocity is simulated through the inlet. Varied air velocity is 0.5 m/s, 0.1 m/s, 1.5 m/s, 2 m/s, and 2.5 m/s. In the storage box at the edge, the air velocity is about twice as high as in the storage box at the centre. The flow patterns in the ripples of the onion stack indicate connections with each other at varying air velocities depending on the small size of the ripples in a stack. Increasing the air velocity at the inlet will increase the flow velocity of the air through the edge of the stack and the large gap. However, airflow remains detected at all position measurements even when the air velocity at the inlet is set to 0.5 m/s.

Keywords: Geometric approach · CFD · Onions · Simulation · Air velocity

1 Introduction

Onion (*Allium cepa* L.) is a spice commodity that plays an essential role in the taste of Indonesian cuisine. In 2021, the number of onions produced in Indonesia, recorded by Badan Pusat Statistik (BPS) [1], reached 2 million tons. The figure increased by 10.42% from the previous year of 1.82 million tons. In addition to being seasonal, onions have perishable properties like other horticultural products. Onions with good post-harvest handling can be kept for up to six months. The quality of onions is tried to be maintained so that their economic value does not decrease. The effort to maintain this quality is one of them by paying attention to the storage air conditioning tailored to the onions' characteristics.

J. Sumantyo et al. (Eds.): ICoSIA 2022, ABSR 29, pp. 295–303, 2023.
https://doi.org/10.2991/978-94-6463-122-7_26

In previous studies, measurements of airflow in the cracks of the product were made using a newly developed wireless anemometer [2]. However, measurements take considerable preparation, such as sensor installation, and caution is required to prevent the sensor from physically damaging the product. Airflows in packaging close to the product are also analyzed using computational fluid dynamics (CFD) [3, 4] or by heat transfer using heated measuring spheres [5]. Airflow is one of the branches of fluid dynamics that can be computed using computational fluid dynamics (CFD). The geometry of the storage space and the stored product will influence its airflow patterns. In addition, to provide a detailed analysis of airflow patterns in the gaps between product stacks, measuring the magnitude of the air velocity added to the inlet is necessary.

The relationship between the air near the inlet, outlet, and airflow in the gap of the onion stack inside the storage box remains unknown. Therefore, the studies presented aim to determine airflow distribution in the onion storage room. Subjective measurements with the human senses cannot be made because the measurement point is not located on the surface. Meanwhile, destructive methods require structural changes and even the destruction of products through complex analysis stages that take a long time to complete [6]. Therefore, developing a non-destructive method of measuring airflow at each point is important. In this case, computational fluid dynamics (CFD) is used for simulation purposes. Briefly, CFD is a structured numerical analysis to solve problems related to fluid flow computers. This method requires no physical interaction with the product, and the measurement process is performed relatively. A geometric approach to the stack of onions is used by forming a spherical stack. Various points in the storage box were investigated to find distributed airflow patterns from the inlet to the outlet.

2 Materials and Methods

2.1 Representative Elementary Volume

Representative Elementary Volumes (REVs) were first created to describe the smallest volume at which measurements were made to yield a representative value of the whole property being investigated [7], in this case, is the stack of onions during storage.

2.2 Geometrical Approach

In this study, the stack of local onion products was visualized by the geometric approach of the spherical stack. The built model has a physical variation in size. The size used ranges from 1–3 cm, following the size of onions listed on SNI 3159:2013. The built-in spherical model is arranged in a stacked and random manner, satisfying the size of the storage box as a representative elementary volume (REV).

2.3 Computational Model

The 3D computational model of the onion stack inside the storage box is modelled, as shown in Fig. 1. Each onion is modelled as a sphere and positioned randomly stacked in Fig. 1a. The spherical shape is modelled after 68 pieces. Storage rooms are modelled

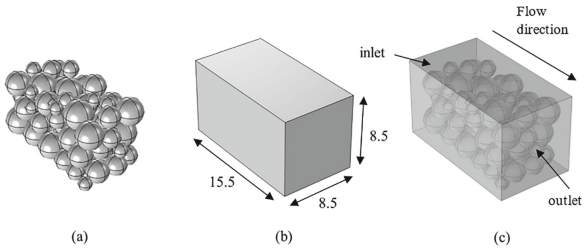

Fig. 1. 3D model: (**a**) a stack of spheres as a representation of onions; (**b**) a storage box model; (**c**) an overall model, storage box with onion geometry inside (all dimensions are in cm).

as rectangular boxes. The box dimensions were 15.5 cm in length, 8.5 cm in width, and 8.5 cm in height. The assumption is that the box's four long sides are closed, with no air flowing in or out. The velocity is assumed to be zero at the boundary [8]. Overall, the combined computational model has a porosity of 59.8%. Compared with previous studies on the total geometry investigated, the result was a random stacking pattern of pear fruit in the box with a porosity of 57.2% [9]. The geometry has 70 domains, 552 boundaries, 830 edges, and 418 vertices.

The 3D modelling was made using COMSOL Multiphysics 5.6. Computation is done by creating a 3D Model Wizard using a single-phase flow study, laminar flow (SPF). The laminar flow interface calculates the velocity and pressure fields for single-phase fluid flows in the laminar flow regime. Physical interfaces support uncompressed and compressed flows at low Mach numbers, usually less than 0.3. It also supports non-Newtonian fluids.

2.4 Mathematical Model

The laminar flow is solved using the Navier-Stokes equation for the conservation of momentum and the continuity equation for the conservation of mass (1)–(3).

$$\rho\left(\frac{\partial u}{\partial t} + u \cdot \nabla u\right) = -\nabla p + \left(\nabla \cdot \left(\mu\left(\nabla u + (\nabla u)^T\right)\right) - \frac{2}{3}\mu(\nabla \cdot u)I\right) + F \quad (1)$$

$$\frac{\partial \rho}{\partial t} + \nabla \cdot (\rho u) = 0 \quad (2)$$

$$\rho \nabla \cdot u = 0 \quad (3)$$

where $\boldsymbol{u}$ is the air velocity (m/s), $\boldsymbol{p}$ is the air pressure (Pa), $\boldsymbol{\rho}$ is the air density (kg/m^3), $\boldsymbol{\mu}$ is the dynamic viscosity of the air (kg/m·s), $\boldsymbol{t}$ is time (s), and $\boldsymbol{T}$ is the air temperature (K).

2.5 Mesh Generation

The pre-processing step for computing field simulation is domain discretization, called mesh generation. Structured grids representing symmetrical 3D flow domains are generated using COMSOL Multiphysics 5.6. The computational domain was discretized

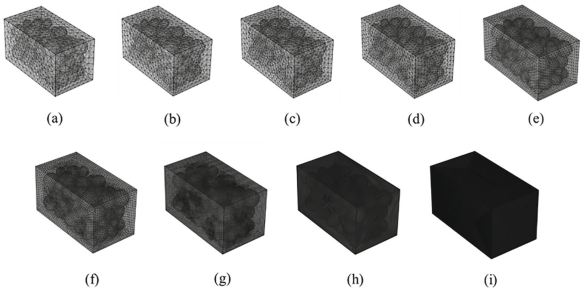

Fig. 2. Structured 3D block mesh generated for fluid dynamics. (**a**) extremely coarse; (**b**) extra coarse; (**c**) coarser; (**d**) coarse; (**e**) normal; (**f**) fine; (**g**) finer; (**h**) extra fine; (**i**) extremely fine.

using a free tetrahedral mesh. After conducting the best meshing, a mesh with a minimum and maximum size of 0.17 cm and 0.57 cm, respectively was used (Fig. 2e). The total number of elements was about 5.59 × 105 for this model of the storage box. A number of these structured meshes were generated to study network independence (Fig. 2). Creating mesh for complex geometries is time-consuming due to the possible to need manually break down the domain into several blocks, depending on the geometry properties.

2.6 Simulation Setup

The simulation was conducted using CFD in COMSOL Multiphysics 5.6. First, the 3D model consists of the onions' geometric approach and storage space. The model size is relatively small because it is used as the actual state's representative elementary volume (REV). The geometry of onions is structured in a stacked box and mesh processing is done. The observations were focused on the airflow in the product gap, so the mesh of the onion geometry was made to Normal size (Fig. 2e).

This study used the laminar flow model to represent airflow in the storage space. In this case, boundary conditions must be specified on each surface of the fluid domain. The boundary conditions used in this model are inlet airflow, outlet airflow, walls, and symmetry. Symmetry boundary conditions are performed on four computational domains with normal velocity components, and gradients assumed to be zero. The airflow inlet is regulated at a constant velocity. Computations are performed with a speed variation of 0.5 m/s to 2.5 m/s.

In previous studies, the variation in air velocity in the product storage space may range from 0.01–2.5 m/s [10]. In addition, there is an inlet temperature of 293.15 K and a pressure of 1 atm. The analysis is performed by processing each mesh and taking velocity values at seven different points inside the storage box. The data was then exported into text format to be analyzed using Microsoft Excel.

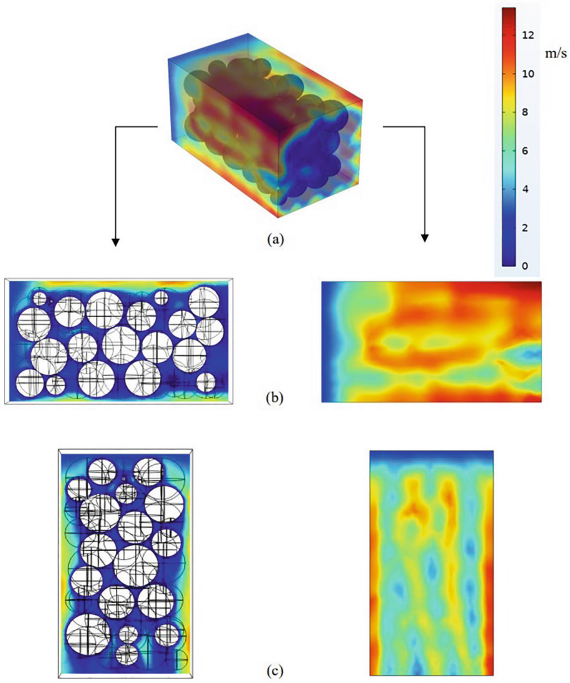

Fig. 3. Air velocity distribution inside the storage box with an inlet of 2.5 m/s. (**a**) Air velocity distribution in the entire airspace; (**b**) Air velocity at the centre from the side view (left) and on the side wall (right); (**c**) Air velocity at the centre looks up (left) and on the upper wall (right).

3 Results and Discussion

3.1 Mesh Suitability

Mesh works by breaking down objects to be simulated into smaller cells so that they can accurately define the geometry of objects. During the meshing process, complex geometric objects are discretized into several cells with different numbers of nodes. These cells have predictable shapes and can correctly capture the physical shape of objects. With high-quality mesh, numerical analysis can be ensured with accuracy and precision [11]. CFD can perform structured, unstructured, or hybrid meshing with either 2D (triangle, quadrilateral) or 3D (tetrahedral, hexahedron) properties and varying densities while meshing structures.

In this study, Tetrahedral 3D meshing was used for the entire geometry. Tetrahedral mesh is more adaptive to a flow domain with a complicated boundary [12]. The selection of the appropriate mesh depends on the processing time and the result of the mesh. Table 1 shows that the higher the mesh quality, the longer it takes. Meshing with high precision takes a long time [13]. If the result of low-quality meshing is equivalent to or nearly equal to the result of high-quality meshing, it needs to be made a new option.

Table 1. Comparison between size, time, and element mesh

Mesh	Time (s)	Elements			Total Elements
		Domain	Boundary	Edge	
Extremely Coarse	3.15	60199	12584	2725	7.55E + 04
Extra Coarse	3.80	85278	16636	3154	1.05E + 05
Coarser	4.70	123555	21780	3656	1.49E + 05
Coarse	6.53	208758	32166	4493	2.45E + 05
Normal	**10.52**	**492387**	**59912**	**6255**	**5.59E + 05**
Fine	20.86	1354214	132696	9390	1.50E + 06
Finer	48.40	4347219	327250	14373	4.69E + 06
Extra Fine	103.48	11005464	671698	19620	1.17E + 07
Extremely Fine	346.32	39553750	1630470	29038	4.12E + 07

Note: Total mesh elements of the sphere is 5.59E + 05.

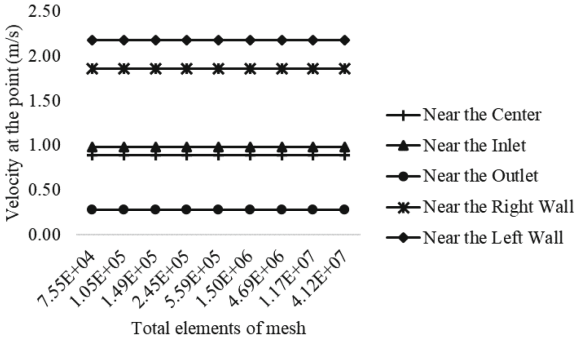

Fig. 4. Air velocity distribution inside the storage box and the geometry gap with an inlet of 1 m/s.

3.1.1 Application of Mesh Divergences

The use of high-quality mesh and the time it takes is comparable to the precision it produces. The total element resulting from the whole geometry is increasingly detailed and accurate. The total mesh elements produced are comparable to the precision of the mesh used. The higher the precision of the mesh, the more elements are formed by the mesh. The lowest total mesh with a value of 7.55 x 10^4 and the highest total element with a value of 4.12 x 10^7 (Table 1).

3.1.2 Effect of Mesh on Air Velocities

The difference in mesh applied resulted in a difference in precision. To improve accuracy and precision in simulations, we can use several meshes with higher resolution on the related geometry so that they have larger gradients of airflow [14].

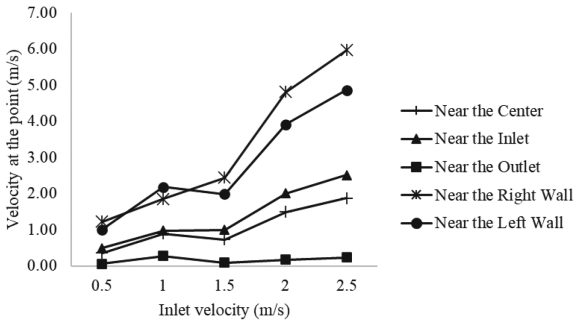

Fig. 5. Air velocities distribution at some points with air velocities variation in the inlet (0.5 m/s; 1 m/s; 1.5 m/s; 2 m/s; 2.5 m/s).

However, from simulations that have been performed with nine different mesh types, it was found that different mesh quality does not affect the distributed air velocity in the storage box. Fig. 4 shows the air velocity value with an inlet of 1 m/s having the same value although given a different mesh.

3.2 Airflow Distribution Within Different Viscosity

Regardless, the air velocity distribution inside the storage box can be measured. The trends are shown in Fig. 5. The measured air velocities at some measurement points increase in proportion to the magnitude of the air velocities exhaled from the inlet point.

That trend shows a definite increase in air velocity at seven measured points. Measurements made at points near the wall (edge side of the storage box) have air velocities 2 to 2.5 times greater than the air velocities introduced through the inlet. This trend can also be seen in Fig. 3 of each slice of the storage box. The air velocity near the outlet at each of these variations is relatively close to 0 m/s.

4 Conclusion

The mesh difference does not affect the distribution values of air velocities inside the storage box and the geometry gap of the onions. The quality of the resulting grid differs real but not with measured air velocity values. Meanwhile, the air velocities simulated at the inlet significantly affect the velocity distribution values of the seven observation points. Therefore, further simulation experiments are required between applying mesh quality with other parameters, measurement variations, and time-based measurements. Further simulations must be performed on all geometries already created on a time-based basis that allows for changes in parameters to the occurrence of time.

Acknowledgments. This paper and the research behind it would not have been possible without the exceptional support of my supervisor, Bayu Nugraha. His enthusiasm, knowledge, and exacting attention to detail have been an inspiration and keep my work to the final draft of this paper. An Nidaa' Fatkhur Rahmah and Devi Priyanti, my research teammate at Universitas Gadjah Mada, have also supporting in wrote this paper. I am also grateful for the insightful comments offered by the anonymous peer reviewers at ICoSIA 2022.

Authors' Contributions. B.N. devised the project, the main conceptual ideas and proof outline. B.N. software and computer simulation coach. B.N. and I.A. carried out the computations. I.A. planned and carried out the simulations. I.A. wrote the manuscript with support from A.N.F.R. and D.P. All author reviewed the final manuscript.

References

1. Badan Pusat Statistik, "Produksi Tanaman Sayuran 2021," https://www.bps.go.id/indicator/55/61/1/produksi-tanaman-sayuran.html, 2021.
2. R. Jedermann, N. Hartgenbusch, M. Borysov, and W. Lang, "Design Parameters for the Housing of Two-Dimensional Air Flow Sensors," IEEE Sens J, vol. 18, no. 24, pp. 10154–10162, Dec. 2018, https://doi.org/10.1109/JSEN.2018.2873896.
3. M. A. Delele, M. E. K. Ngcobo, S. T. Getahun, L. Chen, J. Mellmann, and U. L. Opara, "Studying airflow and heat transfer characteristics of a horticultural produce packaging system using a 3-D CFD model. Part I: Model development and validation," Postharvest Biol Technol, vol. 86, pp. 536–545, Dec. 2013, https://doi.org/10.1016/j.postharvbio.2013.08.014.
4. J. W. Han, C. J. Zhao, X. T. Yang, J. P. Qian, and B. L. Fan, "Computational modeling of airflow and heat transfer in a vented box during cooling: Optimal package design," Appl Therm Eng, vol. 91, pp. 883–893, Dec. 2015, https://doi.org/10.1016/j.applthermaleng.2015.08.060.
5. S. Duret, H. M. Hoang, D. Flick, and O. Laguerre, "Experimental characterization of airflow, heat and mass transfer in a cold room filled with food products," International Journal of Refrigeration, vol. 46, pp. 17–25, 2014, https://doi.org/10.1016/j.ijrefrig.2014.07.008.
6. I. Prabasari, "Comparison of destructive and non destructive method in maturity index of Garcia mangostana," Planta Tropika: Journal of Agro Science, vol. 6, no. 2, 2018, https://doi.org/10.18196/pt.2018.086.100-105.
7. A. Singh, K. Regenauer-Lieb, S. D. C. Walsh, R. T. Armstrong, J. J. M. van Griethuysen, and P. Mostaghimi, "On Representative Elementary Volumes of Grayscale Micro-CT Images of Porous Media," Geophys Res Lett, vol. 47, no. 15, Aug. 2020, https://doi.org/10.1029/2020GL088594.
8. Y. Jiang, B. Li, and J. Chen, "Analysis of the velocity distribution in partially-filled circular pipe employing the principle of maximum entropy," PLoS One, vol. 11, no. 3, Mar. 2016, https://doi.org/10.1371/journal.pone.0151578.
9. M. A. Delele et al., "Spatial distribution of gas concentrations and RQ in a controlled atmosphere storage container with pear fruit in very low oxygen conditions," Postharvest Biol Technol, vol. 156, Oct. 2019, https://doi.org/10.1016/j.postharvbio.2019.05.004.
10. M. A. Delele et al., "Combined discrete element and CFD modelling of airflow through random stacking of horticultural products in vented boxes," J Food Eng, vol. 89, no. 1, pp. 33–41, Nov. 2008, https://doi.org/10.1016/j.jfoodeng.2008.03.026.
11. Y. Qin, "Application of mesh generation technology in bone mechanics research," Journal of Complexity in Health Sciences, vol. 2, no. 1, pp. 23–28, Jun. 2019, https://doi.org/10.21595/chs.2019.20498.
12. S. S. Isukapalli, S. Mazumdar, P. George, B. Wei, B. Jones, and C. P. Weisel, "Computational fluid dynamics modeling of transport and deposition of pesticides in an aircraft cabin," Atmos Environ, vol. 68, pp. 198–207, Apr. 2013, https://doi.org/10.1016/j.atmosenv.2012.11.019.

13. Z. Ali, P. G. Tucker, and S. Shahpar, "Optimal mesh topology generation for CFD," Comput Methods Appl Mech Eng, vol. 317, pp. 431–457, Apr. 2017, https://doi.org/10.1016/j.cma.2016.12.001.
14. M. M. Doustdar and H. Kazemi, "Effects of fixed and dynamic mesh methods on simulation of stepped planing craft," Journal of Ocean Engineering and Science, vol. 4, no. 1, pp. 33–48, Mar. 2019, https://doi.org/10.1016/j.joes.2018.12.005